

**High exchange-bias blocking temperature in an ultrathin amorphous antiferromagnet system**

Jiajun Guo, Xiaonan Zhao, Zhijian Lu, Peng Shi , Yufeng Tian , Yanxue Chen, Shishen Yan, and Lihui Bai \*

*School of Physics, State Key Laboratory of Crystal Materials, Shandong University, 27 Shandan Road, Jinan 250100, China*

Michael Harder 

*Department of Physics, British Columbia Institute of Technology, 3700 Willingdon Avenue, Burnaby, British Columbia, Canada, V5G 3H2*



(Received 23 April 2021; revised 11 July 2021; accepted 23 August 2021; published 1 September 2021)

We experimentally observed an ultrahigh blocking temperature, above 600 K, in an exchange-biased Fe/FeO bilayer after field annealing at 773 K. This is far above the 198 K Néel temperature of bulk FeO. By comparing with an Fe/FeO/Fe trilayer and studying the Fe thickness dependence, we find that the magnetic proximity effect, due to coupling between the Fe layer and the ultrathin amorphous FeO layer, is responsible for the high blocking temperature. The realization of high-temperature exchange bias using an ultrathin antiferromagnet paves the way to further miniaturize magnetic devices for high-information-density applications.

DOI: [10.1103/PhysRevB.104.L100401](https://doi.org/10.1103/PhysRevB.104.L100401)

**Introduction.** The exchange-bias effect in magnetic multilayers produces a shift in the magnetization curve of a soft ferromagnet (FM) when exchange coupled to a hard antiferromagnet (AFM) [1,2]. In modern magnetic devices, such as magnetic random access memory (MRAM) and spin valves, exchange bias is crucial as it enables pinning and stabilization of the magnetization configuration [3–6]. However, exchange bias occurs below a blocking temperature  $T_B$ , and therefore only a few FM/AFM bilayers, such as FeCo/IrMn, are appropriate for applications at room temperature [7]. Furthermore, since  $T_B$  decreases with decreasing thickness of the thin AFM layer [8–10], typically AFM thicknesses exceed 15 nm. This is an obstacle to applications requiring high-density integration, and an open challenge is to realize high  $T_B$  with an ultrathin AFM layer.

When fabricating exchange-biased FM/AFM bilayers, it is necessary to field cool from above the Néel temperature  $T_N$  [1,2]. Since  $T_B$  depends on, and is lower than,  $T_N$  for thin AFM layers [3], increasing  $T_N$  is a necessary step towards increasing  $T_B$ . Previous work has found that  $T_N$  in thin AFM layers can be enhanced by coupling to the adjacent FM layer, for example, in a CoO/Fe<sub>3</sub>O<sub>4</sub> system [10] or Fe<sub>x</sub>Mn<sub>1-x</sub>/Co bilayer [11]. Furthermore, when an FeO layer is embedded between two Fe layers [12],  $T_N$  is drastically increased up to 800 K, greatly exceeding the bulk FeO value of 198 K [13]. These observations suggest that a high  $T_B$  can be achieved by increasing  $T_N$  through interlayer FM/AFM coupling. One may therefore expect the magnetic proximity effect at the interface, which can increase  $T_N$  [14,15], to play a role in achieving high  $T_B$ . However, since a large number of AFM spins are required to observe the magnetic proximity effect, while only a few uncompensated AFM spins couple with the FM spins in an exchange-biased system [15],  $T_B$  enhancement

via the magnetic proximity effect in bulk FM/AFM systems has not been realized.

In this Research Letter we experimentally demonstrate high  $T_B$ , above 600 K, in an exchange-biased Fe/FeO bilayer using a 2-nm-thick amorphous FeO layer. To achieve this result, we find that field annealing at high temperature (773 K) is crucial. The origin of the increased  $T_B$  is the large number of uncompensated spins provided by the amorphous FeO layer, which is verified by comparing the Fe/FeO behavior with an Fe/FeO/Fe trilayer. The fact that  $T_B$  is strongly dependent on the Fe thickness also indicates that the coupling between the FeO and Fe layers increases the effective  $T_N$  via the magnetic proximity effect. Therefore we demonstrate that the magnetic proximity effect in an amorphous AFM exchange-biased system can produce a high  $T_B$ . This understanding may provide a way to further miniaturize magnetic devices for the purpose of high-density integration.

**Introducing exchange bias in the Fe/FeO bilayer.** To fabricate our bilayers, Fe films were grown by dc magnetron sputtering on silicon substrates with a 3-nm Ta buffer layer at room temperature under an Ar pressure of 0.5 Pa. A 2-nm-thick amorphous FeO layer was prepared by exposing the Fe films to high-purity oxygen gas with a pressure of 1 Pa [16]. The sample thickness was estimated by the growth rate, measured using a cross-sectional transmission electron micrograph (TEM). The uniform thickness of the FeO layer was confirmed by an energy-dispersive x-ray spectroscopy (EDS) elemental mapping of the Fe/FeO cross section. A more detailed discussion can be found in the Supplemental Material [17]. All samples were protected from air contamination by 3 nm of Pt. The amorphous nature of the FeO was confirmed using a high-resolution cross-sectional TEM, as shown in the inset of Fig. 1(a). While lattice fringes can be observed in the Fe layer, they do not appear in the 2-nm FeO layer, indicating a typical amorphous structure consistent with the disordered crystalline state of saturated native iron oxide films, which has been studied by x-ray absorption spectroscopy (XAS)

\*lhbai@sdu.edu.cn

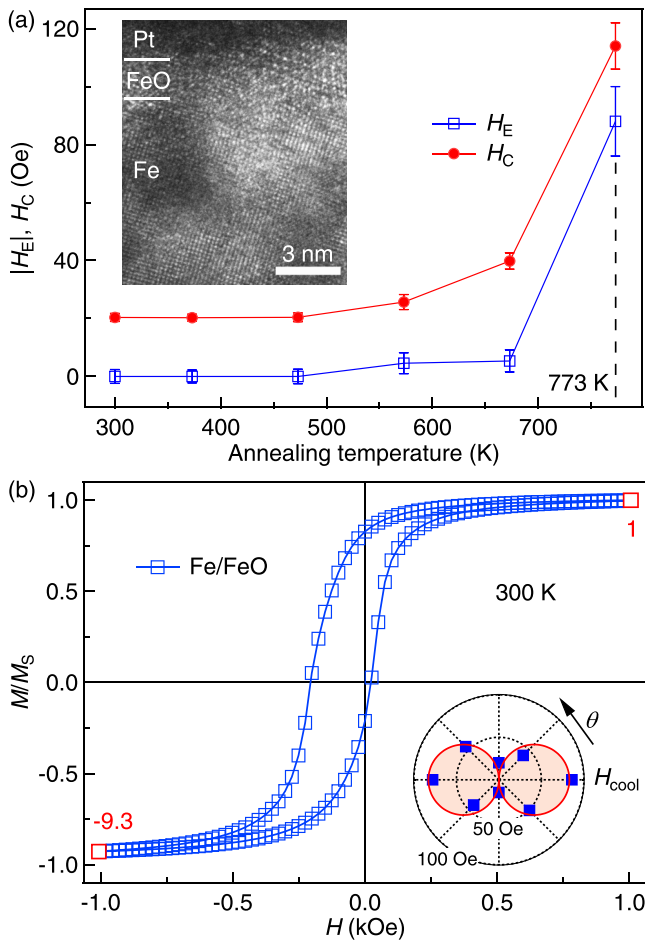


FIG. 1. (a) The field annealing temperature dependence of the magnitude of the exchange-bias field  $|H_E|$  and the coercivity  $H_C$  for an Fe(18 nm)/FeO(2 nm) bilayer at room temperature. The inset shows a high-resolution TEM cross section of the Fe/FeO bilayer after field annealing at 773 K. (b) Hysteresis loop of an Fe(18 nm)/FeO(2 nm) bilayer at room temperature (300 K). The inset shows  $|H_E|$  vs the angle  $\theta$  between the in-plane applied magnetic field and the cooling field  $H_{cool}$ . Blue filled squares represent the measured  $|H_E|$  values, and the red curve depicts the  $|\cos \theta|$  dependence of  $|H_E|$ .

[16]. The amorphous structure of the FeO layer was further confirmed by grazing incidence x-ray reflectometry (GIXRD) and a fast Fourier transform (FFT) analysis of the TEM image. For further details, see the Supplemental Material [17].

To introduce an exchange-bias effect, all the Fe/FeO bilayers (the FeO layer had a constant thickness of 2 nm, and the Fe layer thickness ranged from 2 to 18 nm) were annealed at 773 K for 30 min in a vacuum furnace under a 6 kOe magnetic field. The Fe/FeO bilayers were subsequently cooled to room temperature in a 6 kOe magnetic field (the magnetic cooling field). Magnetic measurements were performed using a Quantum Design superconducting quantum interference device (SQUID) magnetometer. The main characteristics of the exchange-bias effect are a shift in the exchange-bias field  $H_E$  of the hysteresis loop along the field axis and an increase of the coercivity  $H_C$ .  $H_E$  and  $H_C$  are calculated according to  $H_E = -(H_{c1} + H_{c2})/2$  and  $H_C = |H_{c1} - H_{c2}|/2$ , where  $H_{c1}$

and  $H_{c2}$  are the coercive fields of the left and right branches in the hysteresis loop, respectively. For annealing temperatures below 773 K we observe no clear hysteresis loop shift or increase in the coercive field of the Fe(18 nm)/FeO(2 nm) bilayer at room temperature, as shown in Fig. 1(a). Furthermore, we observed no hysteresis loop shift in an unannealed Fe(18 nm)/FeO(2 nm) bilayer even at a temperature of 5 K [17]. This indicates that the effective  $T_N$  of the amorphous FeO layer is around 773 K, since an annealing temperature above  $T_N$  is necessary to produce the exchange bias in FM/AFM bilayers [3]. This enhanced  $T_N$  is consistent with the expected enhancement due to magnetic coupling at the Fe/FeO interface [12].

The most prominent signature of the exchange-bias effect, a horizontal hysteresis loop shift, can be seen in Fig. 1(b), measured in an Fe(18 nm)/FeO(2 nm) bilayer at room temperature (300 K) after field annealing at 773 K. In addition to the horizontal shift, a hysteresis loop at room temperature also exhibits a vertical shift of 3.5% of the saturation magnetization  $M_S$ . Such a vertical shift is due to pinned moments that are not rotated in the applied field [18–20], indicating a large number of pinned uncompensated spins in the AFM layer. It is known that an FeO layer obtained by *in situ* oxidation has a disordered structure with additional Fe ions (such as  $Fe^{3+}$  sites) [16]. These Fe ions are not an integral part of the AFM sublattice, leading to a large number of uncompensated spins in the FeO layer. The magnitude of the exchange-bias field  $|H_E|$  versus the angle  $\theta$ , between the in-plane applied magnetic field and the cooling field  $H_{cool}$ , is shown in the inset of Fig. 1(b). The strength of  $H_E$  is proportional to  $|\cos \theta|$ , which characterizes the unidirectional anisotropy of the Fe/FeO bilayer [21,22]. The data shown in Fig. 1(b) demonstrate the exchange-bias effect in the Fe/FeO bilayer at room temperature.

*Role of amorphous FeO in achieving high  $T_B$ .* The amorphous nature of the FeO layer plays an important role in the high  $T_B$  of the Fe/FeO bilayer. This can be seen by comparing the  $H_E$  and  $H_C$  temperature dependence of an Fe/FeO bilayer and an Fe/FeO/Fe trilayer. Data extracted from the Fe(18 nm)/FeO(2 nm) bilayer (annealed at 773 K) hysteresis are shown as blue squares in Figs. 2(a) and 2(b), between 300 and 750 K. The magnitude of  $H_E$  decreases with increasing temperature and vanishes at a  $T_B$  of 700 K, which is much higher than the  $T_N$  of 198 K in bulk FeO [13]. The sign of  $H_E$  changed just below  $T_B$ , and the maximum negative value of  $H_E$  occurs at the same temperature as the peak in  $H_C$ . This phenomenon may be attributed to the long-ranged oscillatory Ruderman-Kittel-Kasuya-Yosida (RKKY) coupling of uncompensated spins deep within the amorphous FeO layer, which also has been observed in Co/CuMn bilayers (a spin-glass exchange-bias system) near 15 K [23].

The high  $T_B$ , and the sign change of  $H_E$  accompanied by a peak in  $H_C$ , all vanish with the deposition of a second Fe layer on the Fe/FeO bilayer. As shown by the red circles in Fig. 2, for an Fe(18 nm)/FeO(2 nm)/Fe(1.6 nm) trilayer (which was also field cooled from 773 K), the magnitudes of  $H_E$  and  $H_C$  decrease with increasing measurement temperature, indicating a  $T_B$  of 10 K, similar to the previously reported value of 30 K in an Fe/FeO/Fe trilayer [12]. Furthermore, in contrast to the Fe/FeO bilayer, no clear vertical

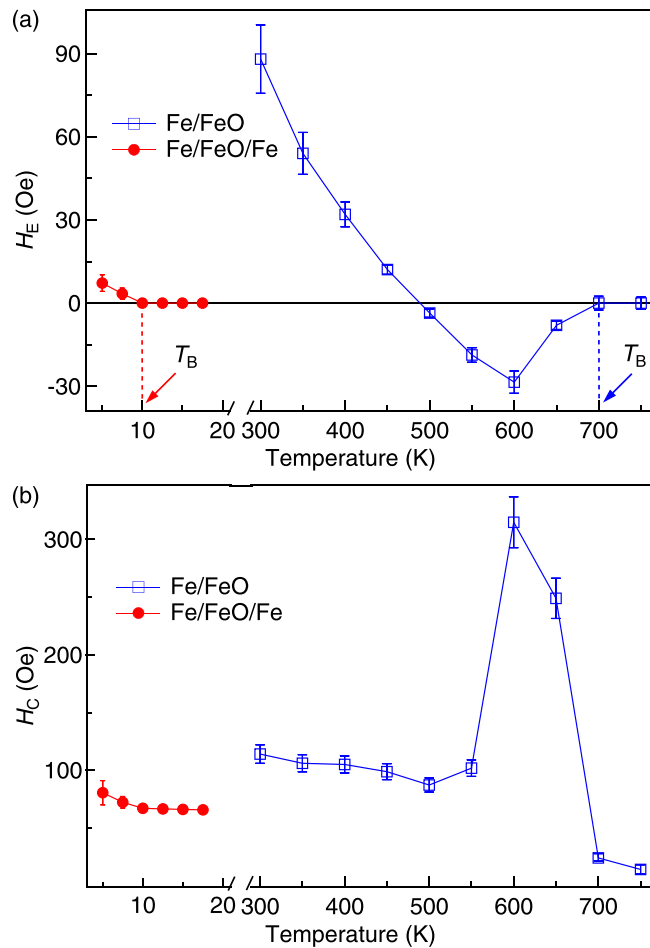


FIG. 2. Temperature dependence of the (a) exchange-bias field  $H_E$  and (b) coercivity  $H_C$  of the Fe(18 nm)/FeO(2 nm) bilayer and the Fe(18 nm)/FeO(2 nm)/Fe(1.6 nm) trilayer.

shift can be seen in the hysteresis loop of the Fe/FeO/Fe trilayer at any temperature [17], indicating that the number of uncompensated spins in the Fe/FeO/Fe trilayer is drastically reduced compared with the Fe/FeO bilayer. This is because the deposition of Fe on the Fe/FeO bilayer causes the ultrathin native FeO layer to change from a disordered structure, with additional Fe ions (such as  $\text{Fe}^{3+}$  sites), to an FeO-like structure containing  $\text{Fe}^{2+}$  sites only [16,24]. Unlike a crystallized AFM exchange-biased system, where uncompensated spins only reside at the AFM surface, in an amorphous AFM layer, uncompensated spins also exist in the bulk [20]. The larger number of uncompensated spins in the AFM layer, which can couple to the FM layer, leads to a magnetic proximity effect in the FM/AFM system [15], drastically increasing the  $T_N$  of the amorphous AFM layer. Therefore the amorphous FeO layer, with its large number of uncompensated spins, plays an important role in the high  $T_B$  observed in the Fe/FeO bilayer.

**Fe thickness dependence of  $T_B$ .** The  $H_E$  and  $H_C$  temperature dependence in the Fe/FeO bilayer was measured for Fe thicknesses between 14 and 2 nm, as shown in Fig. 3. In all samples the FeO layer had a constant thickness of 2 nm. For all Fe thicknesses the magnitude of  $H_E$  was found to decrease with increasing temperature, with  $H_E \rightarrow 0$  defining  $T_B$ . As seen by

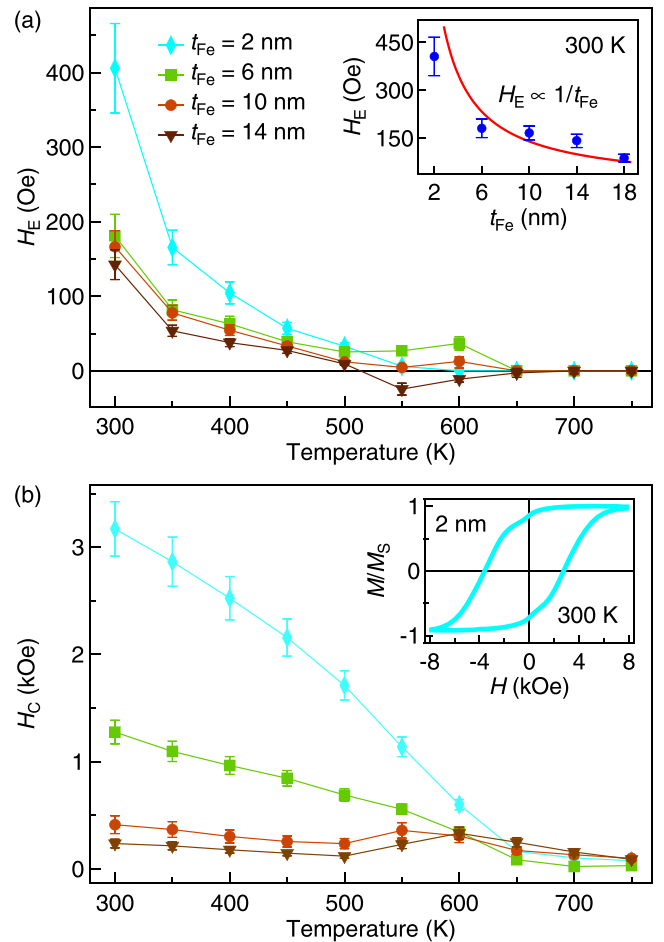


FIG. 3. Temperature dependence of (a)  $H_E$  and (b)  $H_C$  in Fe/FeO bilayers with Fe thickness  $t_{\text{Fe}}$  ranging from 2 to 14 nm. The inset in (a) shows  $H_E$  as a function of  $t_{\text{Fe}}$  in the Fe/FeO bilayer at room temperature (300 K). The inset in (b) shows the hysteresis loop of the Fe(2 nm)/FeO(2 nm) bilayer at room temperature (300 K).

comparing the curves in Fig. 3(a), the high  $T_B$  observed in the Fe/FeO bilayer is strongly dependent on the Fe layer, decreasing by up to 100 K when  $t_{\text{Fe}}$  was reduced from 14 to 2 nm. As shown in the inset of Fig. 3(a),  $H_E$  in the Fe/FeO bilayer is inversely proportional to  $t_{\text{Fe}}$ , decreasing with increasing  $t_{\text{Fe}}$  at room temperature (300 K). This behavior has been observed in most FM/AFM exchange-bias systems [1,2]. In Fig. 3(b) we see that  $H_C$  also decreased with increasing temperature, approaching the value of a single Fe layer (about 23 Oe in our study) at temperatures above  $T_B$ . The temperature dependence of  $H_C$  is more obvious for smaller  $t_{\text{Fe}}$ ; as shown in the inset of Fig. 3(b), a broad hysteresis loop with a  $H_C$  of 3.17 kOe is observed in the Fe(2 nm)/FeO(2 nm) bilayer at room temperature. The enhancement of  $H_C$  compared with a single FM layer at temperatures below  $T_B$  has been observed in most FM/AFM exchange-bias systems and is generally believed to result from exchange coupling of the FM to the larger-anisotropy AFM [1–3].

Figure 4(a) shows the saturation magnetization as a function of temperature,  $M(T)$ , for unannealed Fe/FeO bilayers with different  $t_{\text{Fe}}$  (2–18 nm). The applied magnetic field for

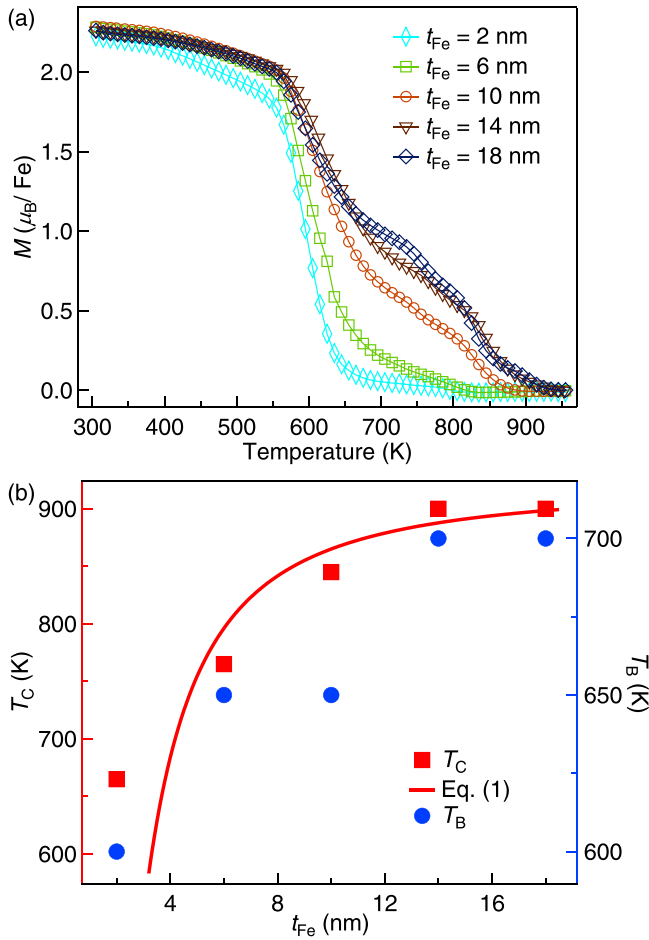


FIG. 4. (a) Temperature dependence of the magnetization  $M(T)$  in Fe/FeO bilayers, for  $t_{\text{Fe}}$  from 2 to 18 nm. (b)  $t_{\text{Fe}}$  evolution of  $T_C$  and  $T_B$  in the Fe/FeO bilayers. The solid line is plotted according to Eq. (1).

these measurements was 200 Oe, which is high enough to saturate all the samples. Since annealing is not necessary to produce the magnetic proximity effect [14,15,25,26], the  $M(T)$  curves of the Fe layer are still influenced by coupling to the FeO layer, even for unannealed Fe/FeO bilayers. From the magnetization curves we can determine the Curie temperature  $T_C$  of all samples (since the uncompensated spins in the FeO layer have a small magnetization contribution). As  $t_{\text{Fe}}$  is reduced, the Curie temperature progressively decreases. The downward shift in  $T_C$  with decreasing thickness is the result of finite-size scaling due to the limitation in the correlation length as the film thickness becomes smaller than the bulk correlation length [27–29]. The correlation length has a power-law temperature dependence,  $\xi(T) = \xi_0[1 - T/T_C(\infty)]^{-1/\lambda}$ , where  $\xi_0$  is the extrapolated correlation length at  $T = 0$  K,  $T_C(\infty)$  is the bulk Curie temperature, and  $\lambda$  is the shift exponent for the finite-size scaling. It follows then that the Curie temperature of a thin layer of thickness  $t$  varies as

$$\frac{T_C(\infty) - T_C}{T_C(\infty)} = \left(\frac{t}{\xi_0}\right)^{-\lambda}. \quad (1)$$

$T_C$  as a function of  $t_{\text{Fe}}$  in the Fe/FeO bilayer can be described by Eq. (1) as shown in Fig. 4(b), with  $\lambda = 1.59$ ,  $T_C(\infty) = 920$  K, and  $\xi_0 = 1.7$  nm, where all parameters have been treated as fit coefficients. The value of  $\lambda = 1.59$  is in agreement with the value of  $\lambda = 1.5584$  for Ising systems [30], while the value of  $T_C(\infty) = 920$  K is close to the 1045 K bulk Curie temperature of Fe [31].  $\xi_0 = 1.7$  nm is quite close to the values of  $\xi_0 = 1.8$  nm for AFM CoO [28] and  $\xi_0 = 1.9$  nm for spin-glass CuMn [32] but is much larger than the angstrom order of magnitude for Fe thin films [33]. The large value of  $\xi_0$  leads to a significant decrease in  $T_C$ , which can be observed even for  $t_{\text{Fe}} = 6$  nm, as shown in Fig. 4(b). This is in contrast to single Fe films, where  $T_C$  does not deviate from the bulk value until the films are only a few atomic layers thick [33–36]. This nanometer enhanced correlation length can be attributed to coupling between the Fe layer and the adjacent amorphous FeO layer, which also has been observed in Fe/Fe<sub>0.32</sub>V<sub>0.68</sub> superlattices [37].

Uncompensated spins exist not only at the surface of the amorphous FeO layer but also in the bulk [20]. Furthermore, since the 2-nm-thick amorphous FeO layer is smaller than the 3.5-nm FM/AFM interaction length [38], all of the uncompensated spins in the amorphous FeO layer can couple with the Fe layer. The large number of AFM spins coupled to the FM layer leads to a large proximity effect in the Fe/FeO bilayer [15], drastically increasing the effective  $T_N$  of FeO. As a result, an obviously enhanced  $T_B$  can be observed in the Fe/FeO bilayers as shown in Figs. 2 and 3. Furthermore, since this high  $T_B$  depends on the magnetic ordering of the Fe layer,  $T_B$  tracks  $T_C$ , and they both decrease as  $t_{\text{Fe}}$  decreases, as shown in Fig. 4(b). The  $t_{\text{Fe}}$  dependence of  $T_B$  is also evidence that the magnetic proximity effect is responsible for the high  $T_B$ . Using mean-field theory [39], the ordering temperatures ( $T_C$  or  $T_N$ ) approach each other as a function of the relative Fe and FeO thicknesses. Since the FeO layer had a constant thickness, changes in  $t_{\text{Fe}}$  influence the effective  $T_N$  of the amorphous FeO layer. As a result, the  $T_B$  of the Fe/FeO bilayer also changes with  $t_{\text{Fe}}$ , indicating that the magnetic proximity effect is responsible for the high  $T_B$ .

When compared with other high- $T_B$  exchange-biased systems [40–48], the 2-nm amorphous FeO thickness reported here is the smallest by a prominent margin (see Fig. 5). Most of the high- $T_B$  materials that have been reported are Mn alloys where the high  $T_B$  originates from a high bulk AFM magnetic ordering temperature. However, the  $T_B$  of these materials usually decreases as the AFM thickness decreases, while  $T_N$  does not change. For example, neutron diffraction studies of MgO(3 nm)/CoO(3 nm) [49] have shown that  $T_N = 305 \pm 10$  K. Therefore  $T_B$  is much lower than the bulk  $T_N$  for very thin AFM layers in these systems [8,9]. It has been suggested that the  $T_B$  reduction is related to a weakening of the spin-spin interaction in the thin AFM layer [50]. In contrast, amorphous materials, which are highly uniform and free of point defects, have disordered atomic structures that can modulate the atomic specific density, resulting in regions of larger exchange coupling, making them ideal for magnetic heterostructures [51–55]. Moreover, since the magnetic ordering depends on the  $T_C$  of the Fe layer, the amorphous FeO can have a large effective  $T_N$  at low thickness. Therefore a large  $T_B$  can be expected in exchange-biased systems using an

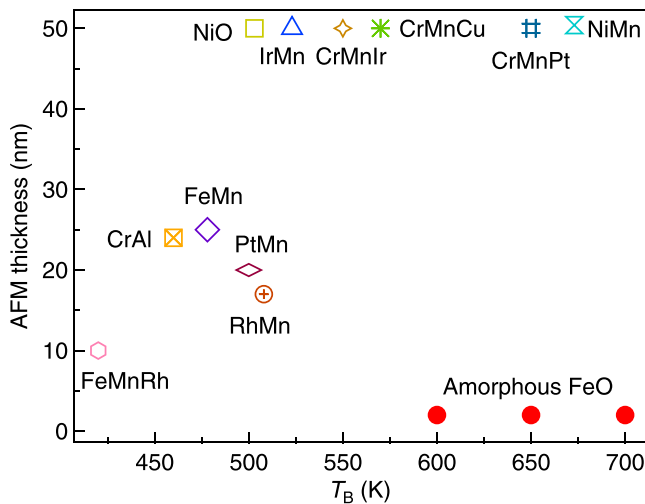


FIG. 5. Comparison of blocking temperature  $T_B$  and AFM thickness in the Fe/FeO bilayer with previously reported data for high- $T_B$  exchange-biased systems [40–48].

ultrathin FeO film. In more general terms, an ultrathin FeO layer obtained by exposure of an Fe film to oxygen gas can induce a large  $T_B$  far greater than room temperature and can lead to the realization of high  $T_B$  in ultrathin metal oxide films, such as NiO, CoO, and  $\text{Cr}_2\text{O}_3$ .

*Conclusions.* In summary, we experimentally demonstrated a high exchange-bias blocking temperature with an ultrathin amorphous FeO layer on an Fe layer. We have outlined the key process of high-temperature annealing to achieve the high blocking temperature, which might be useful in practical applications. Moreover, this work lays the groundwork for future studies, such as the exploration of the magnetic proximity effect to enhance the blocking temperature of various miniature spintronic devices.

*Acknowledgments.* This work is supported by the National Natural Science Foundation of China (NSFC Grant No. 11774200), the Shandong Provincial Natural Science Foundation (Grant No. ZR2019JQ02), and the Youth Interdisciplinary Science and Innovative Research Groups of Shandong University. M.H. is supported by Institute Research Funds from the British Columbia Institute of Technology.

- [1] J. Nogués and I. K. Schuller, *J. Magn. Magn. Mater.* **192**, 203 (1999).
- [2] A. E. Berkowitz and K. Takano, *J. Magn. Magn. Mater.* **200**, 552 (1999).
- [3] J. Nogués, J. Sort, V. Langlais, V. Skumryev, S. Surinach, J. Muñoz, and M. Baro, *Phys. Rep.* **422**, 65 (2005).
- [4] A. D. Kent and D. C. Worledge, *Nat. Nanotechnol.* **10**, 187 (2015).
- [5] W. Zhang and K. M. Krishnan, *Mater. Sci. Eng., R* **105**, 1 (2016).
- [6] P.-H. Lin, B.-Y. Yang, M.-H. Tsai, P.-C. Chen, K.-F. Huang, H.-H. Lin, and C.-H. Lai, *Nat. Mater.* **18**, 335 (2019).
- [7] H. N. Fuke, K. Saito, M. Yoshikawa, H. Iwasaki, and M. Sahashi, *Appl. Phys. Lett.* **75**, 3680 (1999).
- [8] T. Ambrose and C. L. Chien, *J. Appl. Phys. (Melville, NY)* **83**, 6822 (1998).
- [9] Y. J. Tang, D. J. Smith, B. L. Zink, F. Hellman, and A. E. Berkowitz, *Phys. Rev. B* **67**, 054408 (2003).
- [10] P. J. van der Zaag, Y. Ijiri, J. A. Borchers, L. F. Feiner, R. M. Wolf, J. M. Gaines, R. W. Erwin, and M. A. Verheijen, *Phys. Rev. Lett.* **84**, 6102 (2000).
- [11] K. Lenz, S. Zander, and W. Kuch, *Phys. Rev. Lett.* **98**, 237201 (2007).
- [12] S. Couet, K. Schlage, R. Rüffer, S. Stankov, Th. Diederich, B. Laenens, and R. Röhlberger, *Phys. Rev. Lett.* **103**, 097201 (2009).
- [13] K. Koike and T. Furukawa, *Phys. Rev. Lett.* **77**, 3921 (1996).
- [14] R. W. Wang and D. L. Mills, *Phys. Rev. B* **46**, 11681 (1992).
- [15] P. K. Manna and S. M. Yusuf, *Phys. Rep.* **535**, 61 (2014).
- [16] S. Couet, K. Schlage, K. Saksl, and R. Röhlberger, *Phys. Rev. Lett.* **101**, 056101 (2008).
- [17] See Supplemental Material at <http://link.aps.org/supplemental/10.1103/PhysRevB.104.L100401> for EDS elemental mapping, GIXRD, and FFT analysis of the Fe/FeO bilayer, the hysteresis loop of the unannealed Fe(18 nm)/FeO(2 nm) bilayer at 5 K, and the hysteresis loops of the Fe(18 nm)/FeO(2 nm)/Fe(1.6 nm) trilayer at 5, 7.5, and 10 K.
- [18] J. Nogués, C. Leighton, and I. K. Schuller, *Phys. Rev. B* **61**, 1315 (2000).
- [19] M. Gruyters, *Phys. Rev. Lett.* **95**, 077204 (2005).
- [20] J. Guo, X. Zhao, Z. Lu, P. Shi, Y. Tian, Y. Chen, S. Yan, L. Bai, and M. Harder, *Phys. Rev. B* **103**, 054413 (2021).
- [21] W. H. Meiklejohn and C. P. Bean, *Phys. Rev.* **102**, 1413 (1956).
- [22] N. J. Gökemeijer, T. Ambrose, and C. L. Chien, *Phys. Rev. Lett.* **79**, 4270 (1997).
- [23] M. Ali, P. Adie, C. H. Marrows, D. Greig, B. J. Hickey, and R. L. Stamps, *Nat. Mater.* **6**, 70 (2007).
- [24] G. S. D. Beach, F. T. Parker, D. J. Smith, P. A. Crozier, and A. E. Berkowitz, *Phys. Rev. Lett.* **91**, 267201 (2003).
- [25] P. K. Manna, S. M. Yusuf, M. Basu, and T. Pal, *J. Phys.: Condens. Matter* **23**, 506004 (2011).
- [26] P. Bhatt, A. Kumar, S. S. Meena, M. D. Mukadam, and S. M. Yusuf, *Chem. Phys. Lett.* **651**, 155 (2016).
- [27] M. E. Fisher and M. N. Barber, *Phys. Rev. Lett.* **28**, 1516 (1972).
- [28] T. Ambrose and C. L. Chien, *Phys. Rev. Lett.* **76**, 1743 (1996).
- [29] R. Zhang and R. F. Willis, *Phys. Rev. Lett.* **86**, 2665 (2001).
- [30] A. M. Ferrenberg and D. P. Landau, *Phys. Rev. B* **44**, 5081 (1991).
- [31] M. Pajda, J. Kudrnovský, I. Turek, V. Drchal, and P. Bruno, *Phys. Rev. B* **64**, 174402 (2001).
- [32] A. Gavrin, J. R. Childress, C. L. Chien, B. Martinez, and M. B. Salamon, *Phys. Rev. Lett.* **64**, 2438 (1990).
- [33] X. F. Cui, M. Zhao, and Q. Jiang, *Thin Solid Films* **472**, 328 (2005).
- [34] W. Dürr, M. Taborelli, O. Paul, R. Germar, W. Gudat, D. Pescia, and M. Landolt, *Phys. Rev. Lett.* **62**, 206 (1989).

- [35] C. M. Schneider, P. Bressler, P. Schuster, J. Kirschner, J. J. de Miguel, and R. Miranda, *Phys. Rev. Lett.* **64**, 1059 (1990).
- [36] Z. Q. Qiu, J. Pearson, and S. D. Bader, *Phys. Rev. Lett.* **70**, 1006 (1993).
- [37] H. Palonen, F. Magnus, and B. Hjörvarsson, *Phys. Rev. B* **98**, 144419 (2018).
- [38] V. K. Valev, M. Gruyters, A. Kirilyuk, and T. Rasing, *Phys. Rev. Lett.* **96**, 067206 (2006).
- [39] J. A. Borchers, R. W. Erwin, S. D. Berry, D. M. Lind, J. F. Ankner, E. Lochner, K. A. Shaw, and D. Hilton, *Phys. Rev. B* **51**, 8276 (1995).
- [40] T. Lin, D. Mauri, N. Staud, C. Hwang, J. K. Howard, and G. L. Gorman, *Appl. Phys. Lett.* **65**, 1183 (1994).
- [41] V. Baltz, J. Sort, S. Landis, B. Rodmacq, and B. Dieny, *Phys. Rev. Lett.* **94**, 117201 (2005).
- [42] S. Soeya, T. Imagawa, K. Mitsuoka, and S. Narishige, *J. Appl. Phys. (Melville, NY)* **76**, 5356 (1994).
- [43] G. Choe and S. Gupta, *Appl. Phys. Lett.* **70**, 1766 (1997).
- [44] R. F. C. Farrow, R. F. Marks, S. Gider, A. C. Marley, S. S. P. Parkin, and D. Mauri, *J. Appl. Phys. (Melville, NY)* **81**, 4986 (1997).
- [45] S. Soeya, Hi. Hoshiya, R. Arai, and M. Fuyama, *J. Appl. Phys. (Melville, NY)* **81**, 6488 (1997).
- [46] T. J. Klemmer, V. R. Inturi, M. K. Minor, and J. A. Barnard, *J. Appl. Phys. (Melville, NY)* **70**, 2915 (1997).
- [47] H. C. Tong, M. Lederman, W. Jensen, M. Tan, D. Ravipati, S. Yuan, P. Thayamballi, D. Wagner, B. Huang, M. Zhao, P. Rana, W. Chen, L. Miloslavsky, D. O’Kane, R. Rottmayer, and M. Dugas, *IEEE Trans. Magn.* **33**, 2884 (1997).
- [48] A. Veloso, P. P. Freitas, N. J. Oliveira, J. Fernandes, and M. Ferreira, *IEEE Trans. Magn.* **34**, 2343 (1998).
- [49] P. J. van der Zaag and J. A. Borchers, in *Magnetic Properties of Antiferromagnetic Oxide Materials*, edited by L. Duó, M. Finazzi, and F. Ciccacci (Wiley-VCH, Weinheim, 2010), Chap. 7, p. 239–300.
- [50] X. Y. Lang, W. T. Zheng, and Q. Jiang, *Nanotechnology* **18**, 155701 (2007).
- [51] H. W. Sheng, W. K. Luo, F. M. Alamgir, J. M. Bai, and E. Ma, *Nature (London)* **439**, 419 (2006).
- [52] P. T. Korelis, A. Liebig, M. Björck, B. Hjörvarsson, H. Lidbaum, K. Leifer, and A. R. Wildes, *Thin Solid Films* **519**, 404 (2010).
- [53] A. Hirata, P. Guan, T. Fujita, Y. Hirotsu, A. Inoue, A. R. Yavari, T. Sakurai, and M. Chen, *Nat. Mater.* **10**, 28 (2011).
- [54] F. Magnus, M. E. Brooks-Bartlett, R. Moubah, R. A. Procter, G. Andersson, T. Hase, S. T. Banks, and B. Hjörvarsson, *Nat. Commun.* **7**, 11931 (2016).
- [55] K. A. Thórarinsdóttir, T. Hase, B. Hjörvarsson, and F. Magnus, *Phys. Rev. B* **103**, 014440 (2021).